

ICING CLOUD MICROSTRUCTURE FROM *IN SITU* MEASUREMENTS

by

J. F. Gayet and M. Bain

(Laboratoire Associé de Météorologie Physique, Université de Clermont II, B.P. 45,
 63170 Aubièrre, France)

ABSTRACT

In several experiments carried out in France, the Republic of the Ivory Coast, and Spain, icing clouds were penetrated at different heights by instrumented research aircraft. This paper describes the range and the frequencies of occurrence of the relevant icing parameters computed on the cloud scale and for different cloud types. Comparisons between microphysical parameters and meteorological radar signatures show the limitations of these radars when used as a means of locating icing clouds.

1. INTRODUCTION

Existing weather statistics demonstrate some significant operational limitations due to icing of aircraft (both aeroplanes and helicopters). Unfortunately, the existing meteorological database is insufficient to describe the operating environment in which aircraft must conduct flights. In addition to the inadequacies of existing atmospheric icing models, a great deal of improvement is needed in short- and long-range forecasting capability. Since 1972, the Laboratoire Associé de Météorologie Physique has been involved in studies on meteorological problems concerning the icing of aircraft. Instrumentation for studying the atmosphere and cloud physics has been extended and improved. It was mounted on a DC7* research aircraft up to 1979 and on a Piper Aztec** aircraft in 1981.

Several experiments were carried out in France during the winter and summer months of 1975 to 1977, in the Republic of the Ivory Coast in October 1977, and in Spain during the winter and spring months of 1979 and 1981. This paper describes the range of the relevant icing parameters measured during the first exploratory experiments in France and the Ivory Coast, and a statistical analysis of the icing cloud microstructure in Spain, where the data were better documented. Some comparisons between microphysical parameters and radar echo signatures are also described to give the limitations of meteorological radar when it is used as a means of locating icing clouds.

* The DC7 aircraft was sponsored and operated by the Direction des Recherches Etudes et Techniques and by the Centre d'Essais en Vol in Brétigny, France.

** The Piper Aztec aircraft is sponsored and operated by the Météorologie Nationale, France.

2. CLOUD PHYSICS INSTRUMENTATION

The available instrumentation on the two aircraft is described in Table I. The spatial resolution of the tape-recorded data was about 100 m for all the parameters and for both aircraft. A more

TABLE I. AIRCRAFT INSTRUMENTATION

Instrumentation	Type of aircraft		
	DC7 (before 1979)	DC7 (during 1979)	Piper Aztec (1981)
PMS ASSP-100, 3<D<45 μm	X		
PMS FSSP-100, 3<D<45 μm		X	X
PMS 1D-C, 20<D<300 μm	X	X	
PMS 1D-P, 300<D<4500 μm	X	X	
PMS 2D-C, 25<D<800 μm		X	X
PMS 2D-P, 250<D<6000 μm		X	
Johnson-Williams meter (D<30 μm)		X	X
Total water content probe	X	X	
Icing probe	X	X	
Rosemount temperature probe	X	X	X
Reverse flow temperature probe			X
Dew-point	X	X	X
Pressures (static and dynamic)	X	X	X
3 cm PPI radar	X	X	
Doppler radar	X	X	
Inertial platform		X	
Radio-beacon	X	X	X
Sideslip (attack and yaw angles)	X	X	X
Cameras	X	X	

detailed description of the aircraft instrumentation and the accuracies and limitations of measurements has been discussed in previous papers (Gayet and Friedlander 1979, Gayet 1981, Personne and others 1982).

3. AN ATTEMPT TO QUANTIFY ICING SEVERITY

The intensity of icing can be related to the rate of ice accretion on an ice collector as a function of several parameters: air temperature, supercooled liquid water content, ice content, collection efficiency, and flight speed and duration in the cloud. Qualitative observations made from the DC7 aircraft (100 m s^{-1} cruise speed) show that icing generally occurred in most of the clouds encountered at temperatures < -2 to -3°C . With the Piper Aztec (cruise speed 60 m s^{-1}), the corresponding temperature limit was about -1°C due to a lower dynamic

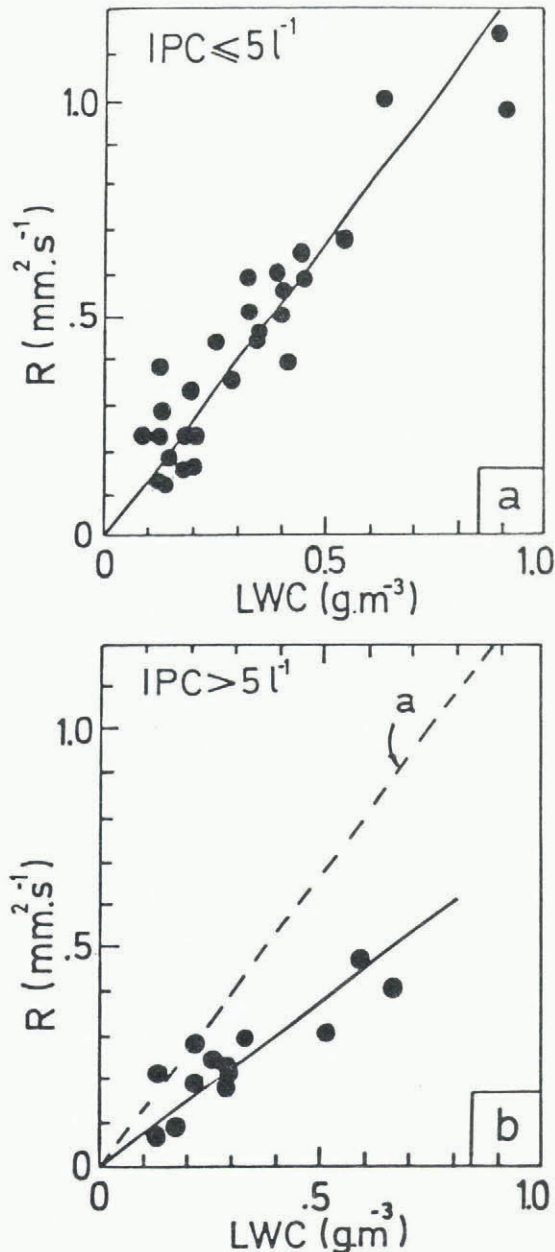


Fig.1. Icing rate R plotted against cloud liquid water content LWC :

- clouds with an ice particle concentration < 5 particles per litre,
- clouds with an ice particle concentration > 5 particles per litre.

heating of the ice probe. Quantitative measurements of the ice profiles on a fixed cylinder (Bain and Gayet 1982) show that increasing liquid water content is generally accompanied by increasing icing intensity. Figure 1(a) is based on the experiment in Spain in spring 1979 and shows the icing rate measured by an icing probe plotted against the liquid water content for several penetrations of stratiform and cumuliform clouds containing a low ice particle concentration (less than 5 particles per litre).

The effect of the ice particles on the icing intensity has not been clarified. Helicopters flying in natural icing conditions have occasionally experienced a sudden rise in the severity of icing (Lake and Bradley 1976). This effect has been explained by the presence of ice crystals in the supercooled clouds. On the contrary, Bain and Gayet (1982) have demonstrated a reduction of the icing rate in cumuliform clouds (near -20°C) containing a noticeable ice particle concentration (more than 5 particles per litre) as shown in Figure 1(b). This figure shows a measured icing rate lower than that in Figure 1(a), possibly because of the erosion caused by the ice particles impinging on the ice deposit.

The overall collection efficiency depends upon several parameters: those related to the air (temperature, density, viscosity), those related to the ice collector (shape and stream velocity), and those related to the cloud (concentration of water/ice, droplet spectrum). Therefore, it is expected that a given type of aircraft will be sensitive to a range of hazards created by icing on the airframe, rotor blades, air intakes, etc., and that different aircraft will experience these problems to varying degrees.

These considerations lead us to present our results in terms of meteorological parameters rather than in terms of icing severities.

4. SOME RESULTS OF THE EXPLORATORY EXPERIMENTS CARRIED OUT IN FRANCE AND THE IVORY COAST

Figure 2(a) shows the mean values of the liquid water content versus the temperature at the penetration level for each traverse of icing clouds performed in France. Two symbols are used to distinguish the cumuliform clouds (\blacktriangle) and the stratiform clouds (\bullet), solid and open symbols corresponding to winter and summer clouds respectively. Figure 2(b) relates to the tropical cumuliform clouds experienced in the Ivory Coast. These two figures show scattered values of the liquid water content for a temperature range between -3 and -15°C .

In France, for all cases studied, the values of the liquid water content ranged from 0.03 to 1.80 g m^{-3} , and 40% of the clouds have a liquid water content $> 0.5 \text{ g m}^{-3}$ (mean value about 0.5 g m^{-3}). The maximum frequency of occurrence of icing clouds is found between -5 and -7°C which corresponds to heights of $2\,700 \text{ m a.s.l.}$ in winter and $4\,300 \text{ m a.s.l.}$ in summer.

Tropical cumuliform clouds are characterized by larger liquid water contents, from 0.2 to 5.8 g m^{-3} (mean value of 1.3 g m^{-3}), and 80% of the clouds have a liquid water content $> 0.5 \text{ g m}^{-3}$. The maximum frequency of occurrence of icing clouds is also found near -6°C , which corresponds to a height of $5\,800 \text{ m a.s.l.}$ The scattered values of the liquid water content are due to the cloud microphysical structure which is variable both spatially and temporally depending on the stage of the life of the cloud. Local values of liquid water content, which were much greater than the values displayed on Figures 2(a) and 2(b), were observed, particularly in tropical clouds where 20 g m^{-3} was measured in an accumulation zone associated with strong updrafts up to 23 m s^{-1} (Gayet and others unpublished).

Qualitative observations of the icing probe made during these cloud penetrations have shown that the

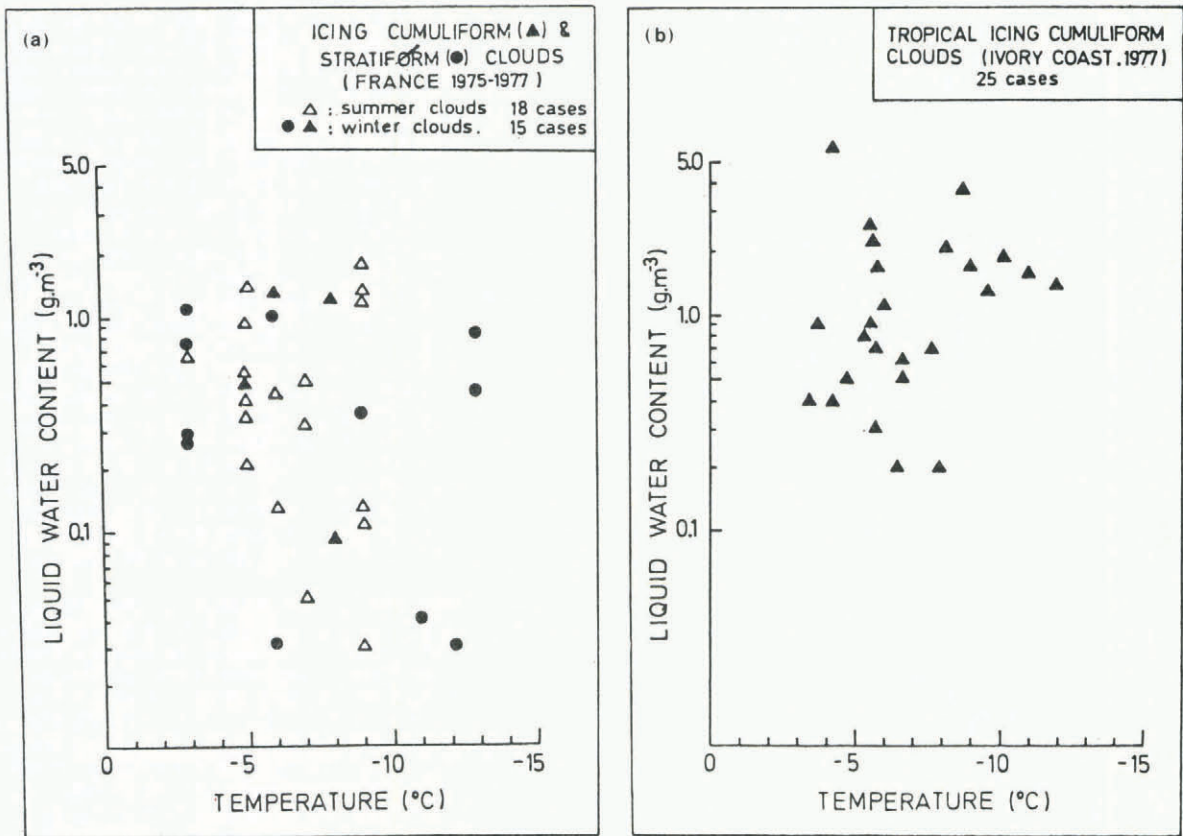


Fig.2. Mean values of liquid water content plotted against temperature at the penetration level: (a) clouds sampled in France, (b) clouds sampled on the Ivory Coast.

icing intensity was not severe despite a large liquid water content due to a loss of water by shedding. Indeed, when the liquid water content is much larger than the critical water content (limit of Ludlam 1951), the supercooled drops are not completely frozen during the impact, the ice grows wet, and run-off of water occurs.

We have also noted that the ice deposit can be partially eroded due to the presence of large particles (graupel or hail).

5. STATISTICAL STUDY OF THE MICROSTRUCTURE OF THE CLOUDS SAMPLED IN SPAIN (1979-1981 EXPERIMENTS)

The results presented in this section have been obtained from data collected in an area in north-west Spain during Site Selection Phase 3 of the World Meteorological Organization Precipitation Enhancement Project (PEP) in 1979 (from 27 March to 4 April) and in 1981 (from 27 March to 16 May). Approximately 650 cloud penetrations at negative temperatures were performed on 33 days; this represents a total in-cloud length of about 3 000 km. Despite the fact that these data are geographically restricted and concern a short period (three months), they give a representative cloud sample including several synoptic situations and are presented as a statistical analysis.

This analysis concerns microphysical and thermodynamical parameters averaged over the cloud penetration. We call penetration a flight in a cloud with a length greater than ~ 1 km (i.e. 10 discrete measurements) and in which the liquid water content is >0.05 g m⁻³ or the ice particle concentration is greater than 0.1 particles per litre. Under these criteria, the median penetration length was 4.5 km and 80% of the penetration lengths were between 1 and 6 km.

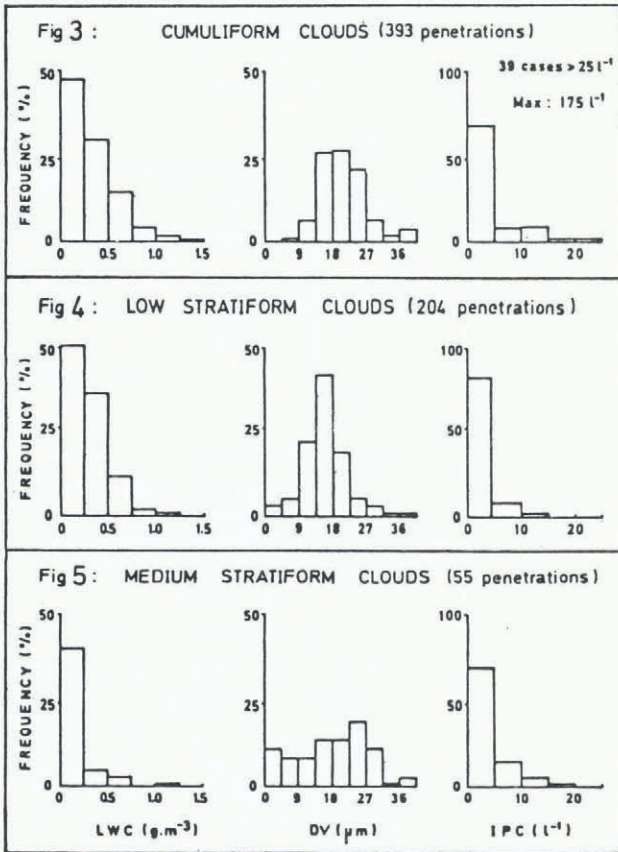
The mean value of the temperature at the penetration level is about -8°C and 13% of penetrations were carried out at a temperature less than -14°C.

Three types of icing cloud are considered: (i) the cumuliform clouds, including cumulus mediocris, winter cumulus congestus and cumulonimbus, (ii) the low stratiform clouds, including stratocumulus and nimbostratus, and (iii) the medium stratiform clouds, including altostratus and altostratus. This cloud classification was made from aircraft observations.

The mean heights of penetration of the different cloud types described above were 2 800, 2 400 and 3 200 m a.s.l. respectively. Due to the sampling period (winter/spring) the cumulus clouds were not very well developed vertically (mean thickness of about 2.1 km) and were found in most cases in complex cloudy situations (embedded convection). The low and medium stratiform clouds had a similar thickness of 1.1 km.

5.1. General characteristics of each cloud category

Figures 3 to 5 display the histograms of the cloud liquid water content, the median volume diameter and the ice particle concentration for the cumuliform, low, and medium stratiform cloud categories, respectively. Table II summarizes the mean values and the standard deviations of the above mentioned parameters together with the horizontal cloud length. Figures 3 to 5 and Table II show that the liquid water contents are similar (0.3 g m⁻³) in cumuliform and low stratiform clouds, but lower (0.18 g m⁻³) in medium stratiform clouds. Noticeable differences appear between the cumuliform and the low stratiform clouds for the median volume diameter (20.8 against 16.1 μm) and for the ice particle concentration (10.1 and 2.9 particles per litre), while intermediate values are found in the medium stratiform clouds (18.1 μm and 7.2 particles per litre,



Figs.3,4,5. Frequency distributions of cloud liquid water content LWC, median volume diameter DV, and ice particle concentration IPC for cumuliform, low and medium stratiform clouds.

respectively). The horizontal cloud length is found to be greater in the medium stratiform clouds (9.3 km), but this parameter does not represent the horizontal cloud extent on account of the flight procedures and the data processing method. Sometimes, stratiform cloud decks exhibit holes which are not taken into account in the evaluation of the microphysical parameters.

5.2. Stratification of the microstructure versus the temperature and the level of penetrations

Figure 6 shows the frequency distributions of the liquid water content plotted against four ranges

of the penetration temperature for all the cloud categories. Table III shows the mean values of the liquid water contents in the same ranges of temperature for the sum of all cloud categories and for each cloud category individually. It appears that the largest liquid water contents are found between -5 and -10°C, particularly for cumuliform clouds (0.41 g m⁻³. This trend is not observed in medium stratiform clouds (maximum values observed for T < -15°C) because most of these clouds occur below -10°C.

Figure 7, with the same representation as Figure 6, shows the frequencies of liquid water content for the four ranges of the penetration level relative to the cloud depth (H = 0 corresponds to the cloud top, and H = 1 to the cloud base). Table IV shows the mean values of liquid water content and median volume diameter in the corresponding relative altitude ranges.

For each cloud category, the greatest values of liquid water content are found three-quarters of the way up from the cloud base (maximum value in cumuliform cloud is 0.37 g m⁻³) and the median volume diameter increases from the base to the top for cumuliform clouds (17.8 to 23 μm).

5.3. Stratification of the microstructure versus the horizontal cloud length and versus the ice particle concentration

The relation between the horizontal extent of the cloud and the extent of icing is an important meteorological parameter for the quantification of icing severity. Figure 8 shows the frequency distributions of the liquid water content plotted against four ranges of the fractional cloud length which contains a liquid water content greater than 0.05 g m⁻³, for all the cloud categories. (For example, when the fractional cloud length is 0.25, this corresponds to 25% of the cloud penetration length, characterized by a liquid water content >0.05 g m⁻³ and the other 75% of the cloud only contains an ice particle concentration greater than 0.1 particles per litre). Table V summarizes the mean values of the horizontal cloud length HCL, in km, and the liquid water content (mean values) in the same ranges as defined in Figure 8 for each cloud category. Figure 8 and Table V suggest that the mean value of the liquid water content increases with the proportion of cloud containing a liquid water content greater than 0.05 g m⁻³ for all cloud categories. The lowest values of liquid water content were found during the longest cloud penetrations (6.2 km) which correspond to the most glaciated clouds. This trend is confirmed in Figure 9 and Table VI where the frequency distributions of the liquid water content are plotted against four ranges of the ice particle concentration.

TABLE II. MICROPHYSICAL CHARACTERISTICS OF THE THREE CLOUD CATEGORIES

	LWC g.m ⁻³		DV μm		IPC l ⁻¹		HCL km	
	MV	SD	MV	SD	MV	SD	MV	SD
Cumuliform	0.33	0.25	20.8	6.9	10.1	21.9	4.5	4.9
Low strat.	0.29	0.19	16.1	5.7	2.9	5.7	3.9	4.6
Med. strat.	0.18	0.27	18.9	9.7	7.2	13.8	6.8	9.3

LWC: liquid water content, DV: median volume diameter, IPC: ice particle concentration, HCL: horizontal cloud extent. MV and SD correspond to the mean values and standard deviations respectively.

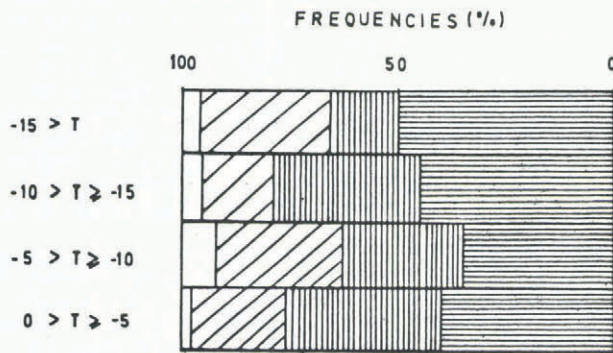


Figure 6

0 < LWC ≤ 0.2 gm⁻³
 0.2 < LWC ≤ 0.4 gm⁻³
 0.4 < LWC ≤ 0.8 gm⁻³
 0.8 < LWC

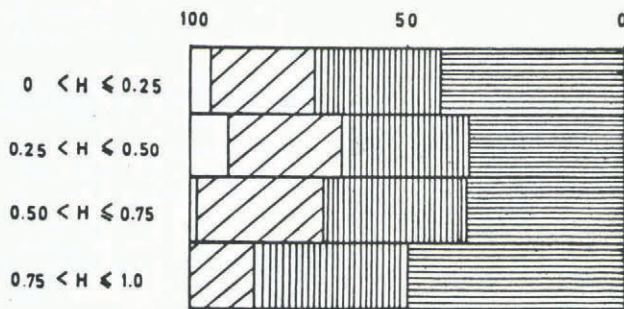


Figure 7

Mean LWC g.m ⁻³			
All categories	Cum.	Low strat.	Med. strat.
.30	.30	—	.36
.27	.27	.31	.21
.36	.41	.31	.11
.29	.33	.26	.12

Table III

All categories		Cum.		Low strat.		Med. strat.	
LWC	DV	LWC	DV	LWC	DV	LWC	DV
.31	19.8	.32	23.0	.29	14.8	.22	20.1
.35	20.0	.37	21.0	.32	17.2	.30	26.6
.30	18.7	.32	19.8	.28	16.6	.18	15.7
.23	17.3	.30	17.8	.22	16.2	.11	18.4

Table IV

Figs.6,7. Frequency distributions of the cloud liquid water content LWC plotted against four ranges of the penetration temperature T (Fig.6) and against four ranges of the penetration level H (Fig.7). Y-axis for Figures 6 and 7 also refer to Tables III and IV respectively (for table legends, see text).

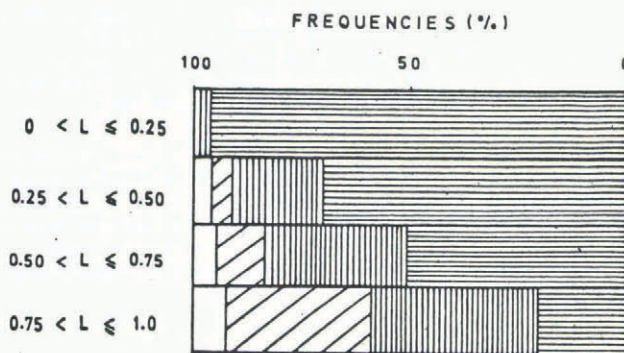


Figure 8

0 < LWC ≤ 0.2 gm⁻³
 0.2 < LWC ≤ 0.4 gm⁻³
 0.4 < LWC ≤ 0.8 gm⁻³
 0.8 < LWC

All categories	Cum.	L.strat.	M.strat.
HCL km	LWC	LWC	LWC
6.2	0.08	0.09	0.05
4.1	0.19	0.21	0.08
4.4	0.25	0.28	0.26
4.2	0.40	0.42	0.32

Table V

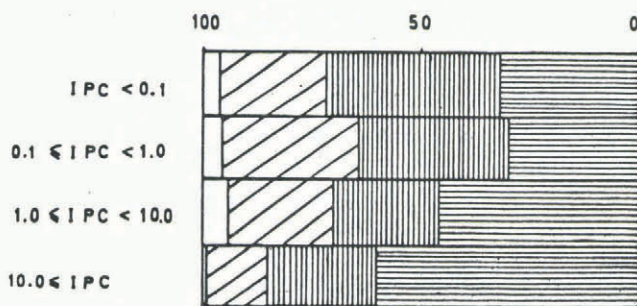


Figure 9

Mean LWC g.m ⁻³			
All categ.	Cum.	L. strat.	M. strat.
0.32	0.37	0.26	0.10
0.36	0.36	0.34	0.45
0.30	0.33	0.31	0.14
0.23	0.25	0.16	0.09

Table VI

Figs.8,9. Frequency distributions of the cloud liquid water content LWC plotted against four ranges of the fractional cloud length L (Fig.8) and against four ranges of the ice particle concentration (Fig.9). Y-axis of Figures 8 and 9 also refer to Tables V and VI respectively (for table legends, see text).

The largest values of liquid water content were found in clouds containing the lowest ice particle concentrations (less than one particle per litre).

6. DETECTION OF THE ICING ZONES FROM CONVENTIONAL METEOROLOGICAL RADARS

The object of this section is to link meteorological radar information with the microphysical parameters and to indicate the limitations of these radars when used as a means of locating icing clouds. To illustrate our purpose, we discuss the results of two successive penetrations carried out with the DC7 aircraft in a growing cumulus congestus cloud at the level 4 300 m a.s.l., with a temperature of -5°C (summer 1976).

During the first traverse, the cloud is a single cell (labelled A) in the growing stage. The variations of the vertical velocity and the microphysical parameters are shown in Figure 10. An updraft of 7 m s⁻¹ is found in the cloud core and the liquid water content reaches 1 g m⁻³. The median volume diameter of the cloud droplet spectrum is about 15 µm and no particles >200 µm are measured. During this penetration no echo was detected by the airborne meteorological radar* (λ = 3 cm, power = 220 kW and range scale = 200 NM, (ø400 km). However a light icing was observed due to a short penetration time

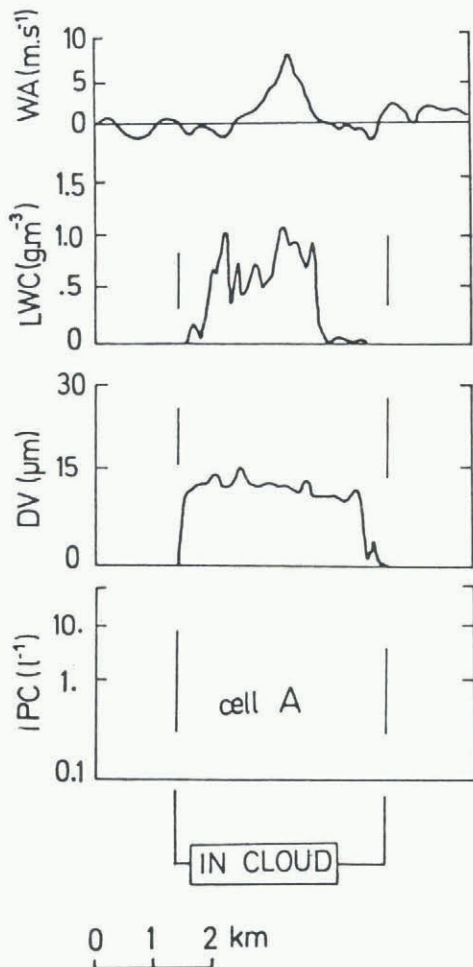


Fig.10. Variation along the flight track of the vertical velocity WA, cloud water content LWC, median volume diameter DV, and ice particle concentration IPC measured during the first cloud penetration (4 300 m a.s.l., temperature of -5°C).

* This is a modified version of the radar type DRAA 2B. In addition to the meteorological information, the radar also provides navigational information.

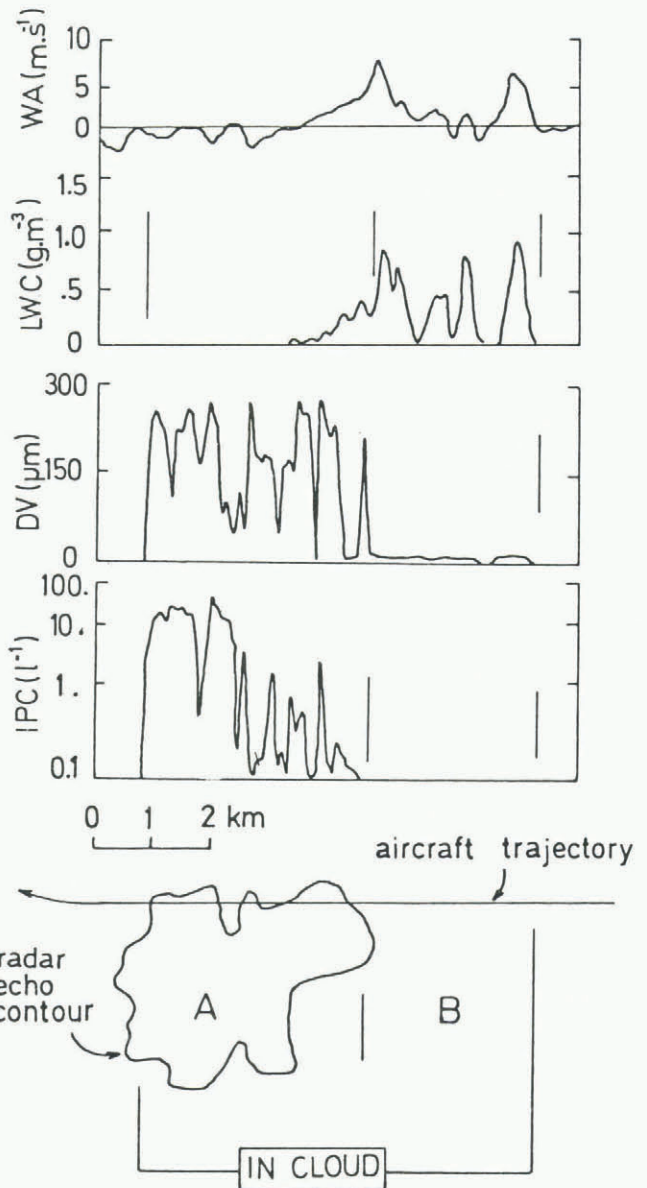


Fig.11. As in Figure 10 for the second cloud penetration. Also shows radar echo contour.

(40 s) and a low mean value of the liquid water content.

Figure 11 represents the evolution of the parameters described above measured ten minutes later, during the second penetration of the same cloud, and the corresponding radar echo contour. This figure reveals sharp discontinuities in the microphysical and dynamical features of the cloud and two cells can be identified: B, which is mainly composed of super-cooled droplets (liquid water content ~1 g m⁻³, median volume diameter ~15 µm), and A (previously sampled) which presents no dynamical activity (vertical velocity approximately zero, low values of liquid water content, noticeable concentration of particles greater than 200 µm (up to 50 particles per litre), median volume diameter (calculated on the ASSP-1D C range 3<D<300 µm) of about 200 µm. Only cell A is correlated with the radar echo contour; however, the icing was judged more severe in cell B (light) than in cell A (trace).

These two examples show that the radar echo signature is a consequence of precipitation particles and that all the icing zones are not related to the radar echo.

The detection threshold depends on the concentration, size, and, also, the nature of these particles (drops or ice crystals). From other investigations and considering the statistically significant minimum concentration of particles measured by the probes (1D-C or 2D-C), a concentration greater than 0.1 particles per litre $>200 \mu\text{m}$ in diameter seems to indicate the lowest limit of detectability with this radar. In the PEP data described in section V, about 27% of the clouds sampled are characterized by very low particle ($D>200 \mu\text{m}$) concentration (<0.1 particles per litre in non-precipitating clouds). This suggests that such a percentage of icing clouds which contain a noticeable liquid water content (mean value: 0.3 g m^{-3} , see Table VI) are not detectable by conventional meteorological radars.

7. CONCLUSIONS

From the data collected during several experiments in France, the Ivory Coast and Spain, the range of the relevant icing parameters are given. Scattered values of liquid water content are found at temperatures between -3 and -15°C due to the spatial and temporal variabilities of the cloud microstructure. Extreme values of liquid water content, up to 20 g m^{-3} were found in tropical cumulonimbus cloud.

In Spain, the icing zones associated with the greatest values of liquid water content were found in a range of temperature between -5 and -10°C and were situated in the upper third quarter of the cloud.

The most extensive clouds, horizontally, and the most glaciated clouds present the lowest mean liquid water content and consequently the lowest icing occurrence. These observations are found to be generally true for the three suggested cloud categories. The detection of icing zones by conventional meteorological radars seems to be ineffective for 27% of the sampled clouds. A specific experiment on the teledetection of icing clouds was carried out last winter (1981-82) in France with an instrumented helicopter (using similar devices to those described here). The results (not yet published) confirm that all icing clouds cannot be detected by conventional meteorological radars. Allowance must therefore be made for this inadequacy when radars are used for forecasting. The alternative is to use other methods.

ACKNOWLEDGEMENTS

The authors would like to express their appreciation to Professor Soulage for his guidance during this study, Professor Coulman for his comments on the manuscript, and Dr Pointin for helpful discussions. Thanks are due to the technical staff at the Laboratoire Associé de Météorologie Physique, Université de Clermont II, and to the crews of the aircraft used in these experiments.

This research was supported by the Direction des Recherches Etudes et Techniques under the contracts 79.34.183 and 80.34.294.

REFERENCES

- Bain M, Gayet J F 1982 Aircraft measurements of icing in supercooled and water droplets/ice crystals clouds. *Journal of Applied Meteorology* 21: 11-21
- Gayet J F 1981 Participation du L.A.M.P. à l'expérience PEP 81. *Laboratoire Associé de Météorologie Physique. Rapport Scientifique* 39
- Gayet J F, Friedlander M 1979 The DC 7 research aircraft of the Centre d'Essais en Vol de Brétigny. *WMO Precipitation Enhancement Project Report* 13
- Gayet J F, Jarmuzynski M, Soulage R G Unpublished. Microstructure of an accumulation zone in a tropical Cb cloud. Presented at the Conference on cloud physics and atmospheric electricity, July 31-August 4, 1978, Issaquah, WA : 318-323 (Preprint)

- Lake H B, Bradley J 1976 The problem of certifying helicopters for flight in icing conditions. *Aeronautical Journal* 80(790): 419-433
- Ludlam S H 1951 The heat economy of a rimed cylinder. *Quarterly Journal of the Royal Meteorological Society* 77: 663-666
- Personne P, Brenguier J L, Pinty J P, Pointin Y 1982 Comparative study and calibration of sensors for the measurement of the liquid water content of clouds with small droplets. *Journal of Applied Meteorology* 21: 73-80